http://mmg.tversu.ru ISSN 2311-1275

Mathematical Modelling and Geometry

Volume 11, No 3, pp. 1 – 20 (2023) doi:10.26456/mmg/2023-1131

Dynamic analysis of a fractional-order delayed SIQR epidemic model for COVID-19 pandemic

Xueyong Zhou[a], **Yaozong Deng**

School of Mathematics and Statistics, Xinyang Normal University,
Xinyang 464000, Henan, P.R. China

e-mail: [a] xueyongzhou@126.com

Received 26 September 2023, in final form 12 October. Published 17 October 2023.

Abstract. In this paper, we build a fractional-order delayed SIQR epidemic model for COVID-19 pandemic. By leveraging the linearization method and the Laplace transform, the characteristic equation of the linearized system corresponding to the model is derived. The relationship between time delay and the stability of the positive equilibrium point is then explored through the examination of the roots of the characteristic equation and the cross-sectional conditions. Furthermore, a formula for calculating the critical value of time delay for the Hopf bifurcation is derived. Finally, suitable system parameters are chosen for numerical simulation to validate the soundness of the theoretical analysis.

Keywords: Fractional calculus; COVID-19 model; Stability; Hopf bifurcation; Delay

1. Introduction

Since COVID-19 was first detected in December 2019, it has rapidly spread across the globe. As of 21 September 2023, over 770 million people have been infected and more than 6 million people have died globally. The rapid spread of COVID-19 poses enormous challenges to both the global healthcare system and economic development, making it one of the worst public health crises of our time. Understanding the dynamics of the spread of COVID-19 is critical to developing effective public health interventions to control its spread. Mathematical modeling provides a valuable tool for studying infectious disease dynamics and predicting the impact of interventions. Currently, a large number of statistical analyses and mathematical models have been developed to investigate the characteristics of epidemic transmission and the effectiveness of prevention and control measures.

Mathematical models play a crucial role in the COVID-19 prevention and control process, mainly in the aspects of prediction and early warning, risk analysis, and the resumption of work and production [1, 2]. Chinazzi et al. [3] employed basic infectious disease models to consider the impact of travel restrictions on population movement and contact, and evaluated the effects of these measures by simulating the process of epidemic transmission. The results demonstrated that travel restrictions can significantly delay the spread rate of the epidemic and reduce the scale of the outbreak. Peeri et al. [4] compared the outbreaks of SARS, MERS, and COVID-19 using infectious disease models based on differential equations, and the results showed that COVID-19 spread faster and on a larger scale than SARS and MERS, but its fatality rate was relatively low. Hiroshi et al. [5] employed Bayesian statistical models to analyze the COVID-19 outbreak on Japanese cruise ships, estimating the proportion of asymptomatic infections and the risk of epidemic transmission. Li et al. [6] discussed how the mathematical model of infectious diseases helps with epidemic prevention and control in the early stages of the COVID-19 pandemic, and its crucial role in major public health emergencies. Based on the established COVID-19 time-lagged non-autonomous infectious disease model, it was revealed that the delay in diagnosis can effectively delay the peak time of infection. This provides an important model reference for the analysis of complex epidemics. There is also a lot of research literature on mathematical models of COVID-19 [7, 8, 9, 10, 11, 12].

Fractional calculus, as an extension of classical integer-order calculus, has emerged as a research hotspot in the field of control [13]. Numerous scientific studies have demonstrated that systems modeled or controlled using fractional calculus exhibit superior performance compared to integer-order systems, such as enhanced robustness and self-noise rejection [14, 15]. Given the current global pandemic of COVID-19, which poses a severe test for human society, it is crucial to delve deeper into the study and application of fractional order theory [16, 17]. This is particularly relevant for various practical issues in mathematics, biology, computer theory, and engineering. By exploring the potential of fractional calculus, we can develop innovative solutions to address complex challenges and improve system performance.

In the realm of infectious disease kinetic research, scientists have discovered that following infection, the human body initially exhibits no symptoms, and only after a certain period of time do some symptoms gradually manifest [18, 19]. Early on, researchers did not consider the delay factor, but later, investigators found that incorporating a time lag (either single or double) leads to more realistic results, such as the latency cycle, immune cycle, and recovery cycle of the disease [20, 21]. This area of research has yielded numerous valuable findings, providing a foundation for more effective prevention and treatment strategies for infectious diseases. By better understanding the dynamics of infection and the impact of time delay, researchers can develop more targeted and efficient interventions to combat infectious diseases [22, 23, 24].

In this paper, based on the existing research results of predecessors, we will focus on the following Caputo fractional order mathematical model for COVID-19 with time delay

$$\begin{cases} D^{\alpha}S(t) = A - \beta S(t-\tau)I(t-\tau) - dS(t), \\ D^{\alpha}I(t) = \beta S(t-\tau)I(t-\tau) - (d+a+\gamma+\sigma)I(t), \\ D^{\alpha}Q(t) = \sigma I(t) - (d+b+p)Q(t), \\ D^{\alpha}R(t) = \gamma I(t) + pQ(t) - dR(t), \end{cases} \tag{1.1}$$

where $\alpha(0 < \alpha \leq 1)$ stands for the order of the equation; $S(t)$, $I(t)$, $Q(t)$, $R(t)$ represents the number of susceptible, infected, quarantined and removed persons at time t, respectively. All parameters are non-negative. A is the recruitment rate of $S(t)$, β denotes the infection coefficient, d represents the natural mortality rate, a denotes the death rate of the disease, σ represents quarantine rate, b denotes the death rate of the disease. γ and p represent the recover rate from group $I(t)$ and $Q(t)$ to $R(t)$, respectively. τ denotes the latent period of the disease.

The initial value condition of model (1.1) is

$$S(\theta) = \varphi_1(\theta) > 0, \quad I(\theta) = \varphi_2(\theta) > 0, \quad Q(0) = Q_0 > 0, \\ R(0) = R_0 > 0, \quad \theta \in [-\tau, 0]. \tag{1.2}$$

In this paper, we will study stability and bifurcation problems for the system of (1.1) using the theory of fractional-order stability and delay differential equations. The paper is organized as follows: Section 2 provides preliminaries, including the definition of the Caputo fractional-order derivative and some useful lemmas. Section 3 presents some basic results, such as the existence and uniqueness, non-negativity, and positive invariance of solutions for system (1.1). In Section 4, we derive local asymptotic stability and bifurcation results for the fractional-order delay COVID-19 model. Section 5 provides numerical examples to verify the obtained theoretical results. Finally, Section 6 concludes the paper.

2. Preliminaries

In this section, we present the definition of Caputo fractional-order derivative and some useful lemmas are recalled for next analysis.

Definition 2.1[13] The fractional integral of order α for a function $f(x)$ is defined as

$$\mathcal{I}^{\alpha} f(x) = \frac{1}{\Gamma(\alpha)} \int_0^x (x-t)^{\alpha-1} f(t) dt,$$

where $x \geq 0$, $\alpha > 0$, $\Gamma(\cdot)$ is the *Gamma* function, $\Gamma(t) = \int_0^{\infty} x^{t-1} e^{-x} dx$.

Definition 2.2[13] The Caputo fractional derivative of order α for the function $f(x) \in C^n([0,\infty),\mathbb{R})$ is defined by

$$D^{\alpha} f(x) = \frac{1}{\Gamma(n-\alpha)} \int_0^x \frac{f^{(n)}(\tau)}{(t-\tau)^{\alpha-n+1}} d\tau,$$

where $x \geq 0$ and n is a positive integer such that $n-1 \leq \alpha < n$.

Furthermore, when $0 < \alpha < 1$,

$$D^{\alpha} f(x) = \frac{1}{\Gamma(1-\alpha)} \int_0^x \frac{f'(\tau)}{(t-\tau)^{\alpha}} d\tau.$$

Lemma 2.1[25] Consider the following fractional order differential system Caputo derivative

$$D^{\alpha} X(t) = \mathcal{A} X(t), \ X(0) = X_0, \tag{2.1}$$

where $\alpha \in (0,1]$, $X(t) \in \mathbb{R}^n$, $X(t) \in \mathbb{R}^n$, $\mathcal{A} \in \mathbb{R}^{n\times n}$. The characteristic equation of system (2.1) is $|s^{\alpha} E - \mathcal{A}| = 0$. If all of the roots of the characteristic equation have negative real parts, then the zero solution of the system is asymptotically stable.

Lemma 2.2[26] Consider the following fractional delay differential system with Caputo derivative

$$D^{\alpha} X(t) = \mathcal{A} X(t) + \mathcal{B} X(t-\tau), \ X(t) = \phi(t), \ t \in [-\tau, 0], \tag{2.2}$$

where $\alpha \in (0,1], X(t) \in \mathbb{R}^n$, $\mathcal{A}, \mathcal{B} \in \mathbb{R}^{n\times n}$ and $\tau \in \mathbb{R}_+^{n\times n}$, then the characteristic equation of system (2.2) is $|s^{\alpha} E - \mathcal{A} - \mathcal{B} e^{-s\tau}| = 0$. If all of the roots of the characteristic equation have negative real parts, then the zero solution of the system is asymptotically stable.

3. Basic results

In the subsequent section, we will delve into the existence and uniqueness of the solution for system (1.1). Additionally, we will establish that the solutions of system (1.1) with initial condition (1.2) are nonnegative and positively invariant.

Theorem 3.1 If $\mathcal{C} \in \mathcal{C}([-\tau, 0], \mathbb{R}_4^+)$ is the continuous function of Banach space and $z_0(t) \in \mathcal{C}$ in an initial condition, then system (1.1) has a unique solution $z(t) \in \Theta$, where $z(t) = (S(t), I(t), Q(t), R(t))$, $\Theta = \{(S(t), I(t), Q(t), R(t)) \in \mathbb{R}^4 | \max\{|S(t)|, |I(t)|, |Q(t)|, |R(t)|\} \le \mathcal{L}\}$.

Proof. Consider the mapping $H(z) = (S(t), I(t), Q(t), R(t))$, where

$$\begin{aligned}
H_1(z(t)) &= A - \beta S(t-\tau)I(t-\tau) - dS(t),\\
H_2(z(t)) &= \beta S(t-\tau)I(t-\tau) - (d+a+\gamma+\sigma)I(t),\\
H_3(z(t)) &= \sigma I(t) - (d+b+p)Q(t),\\
H_4(z(t)) &= \gamma I(t) + pQ(t) - dR(t).
\end{aligned}$$

For any $t_1,\ t_2 \in \Theta$,

$$\begin{aligned}
\|H(z(t_1)) - H(z(t_2))\| &\le \|H_1(z(t_1)) - H_1(z(t_2))\| + \|H_2(z(t_1)) - H_2(z(t_2))\|\\
&\quad + \|H_3(z(t_1)) - H_3(z(t_2))\| + \|H_4(z(t_1)) - H_4(z(t_2))\|\\
&= |\beta S(t_1-\tau)I(t_1-\tau) + dS(t_1) - \beta S(t_2-\tau)I(t_2-\tau) - dS(t_2)|\\
&\quad + |\beta S(t_1-\tau)I(t_1-\tau) - \beta S(t_2-\tau)I(t_2-\tau) - (d+a+\gamma+\sigma)I(t_1)\\
&\qquad\qquad + (d+a+\gamma+\sigma)I(t_2)|\\
&\quad + |\sigma I(t_1) - (d+b+p)Q(t_1) - \sigma I(t_2) + (d+b+p)Q(t_2)|\\
&\quad + |\gamma I(t_1) + pQ(t_1) - dR(t_1) - \gamma I(t_2) - pQ(t_2) + dR(t_2)|\\
&\le (2\beta\mathcal{L} + d)|S(t_1) - S(t_2)| + (d+a+2\gamma+2\sigma)|I(t_1) - I(t_2)|\\
&\quad + (d+b+2p)|Q(t_1) - Q(t_2)| + d|R(t_1) - R(t_2)|\\
&\le \mathcal{M}|z(t_1) - z(t_2)|,
\end{aligned}$$

where $\mathcal{M} = \max\{2\beta\mathcal{L} + d, d+a+2\gamma+2\sigma, d+b+2p, d\}$. Hence, $H(z(t))$ satisfies Lipschitz condition. From Lemma 5 in [27], we can obtain that system (1.1) has a unique solution $z(t)$.

Theorem 3.2 The solutions of system (1.1) with initial condition (1.2) are nonnegative.

Proof. Assume that $\mathbb{R}_+^4 = \{(S, I, Q, R) \in \mathbb{R} : S \ge 0, I \ge 0, Q \ge 0, R \ge 0\}$ is positively invariant. System (1.1) can be written in the vector form

$$D^\alpha X(t) = H(z(t)).$$

Here, $z(t) = (S(t), I(t), Q(t), R(t))^\top$, and

$$H(z(t)) = \begin{bmatrix} A - \beta S(t-\tau)I(t-\tau) - dS(t)\\ \beta S(t-\tau)I(t-\tau) - (d+a+\gamma+\sigma)I(t)\\ \sigma I(t) - (d+b+p)Q(t)\\ \gamma I(t) + pQ(t) - dR(t) \end{bmatrix},$$

$z_0 = (S(\theta), I(\theta), Q(\theta), R(0))^\top \in \mathbb{R}^4_+$. For that, we investigate the direction of the vector field $H(z(t))$ on each coordinate space and see whether the vector field points to the interior of $\mathbb{R}^4_+$. From (1.1), we have

$$\begin{aligned} &D^\alpha S(t)|_{S=0} = A > 0,\\ &D^\alpha I(t)|_{I=0} = 0,\\ &D^\alpha Q(t)|_{Q=0} = \sigma I(t) \geq 0,\\ &D^\alpha R(t)|_{R=0} = \gamma I(t) + pQ(t) \geq 0. \end{aligned} \tag{3.1}$$

From Theorem 1 in [28], Lemma 6 [29] and Eq. (3.1), then the vector field $H(z(t))$ is interior of $\mathbb{R}^4_+$. The solution of (1.1) with initial conditions $z_0 \in \mathbb{R}^4_+$; say $z(t) = z(t, X_0)$, in such a way that $z(t) \in \mathbb{R}^4_+$.

Theorem 3.3 The set $\Omega = \{(S, I, Q, R) \in \mathbb{R}^4_+ | S + I + Q + R \leq \frac{A}{d}\}$ is positively invariant with respect to system (1.1).

Proof. Let $(S(t), I(t), Q(t), R(t))$ be the solution of system (1.1) with initial condition (1.2). Set $N(t) = S(t) + I(t) + Q(t) + R(t)$. From system (1.1), we can obtain

$$\begin{aligned} D^\alpha N(t) &= A - dN(t) - aI(t)\\ &\leq A - dN(t). \end{aligned}$$

Hence,

$$N(t) \leq (-A + N(t))E_\alpha(-dt^\alpha) + A.$$

Obviously, $E_\alpha(-dt^\alpha) \geq 0$. Hence, $N(t) = S(t) + I(t) + Q(t) + R(t) \leq \frac{A}{d}$ when $S(0) + I(0) + Q(0) + R(0) \leq \frac{A}{d}$. And $\Omega = \{(S, I, Q, R) \in \mathbb{R}^4_+ | S + I + Q + R \leq \frac{A}{d}\}$ is positively invariant with respect to system (1.1).

4. Analysis of stability and Hopf bifurcation

The equilibria of system (1.1) are the points of intersections at which $D^\alpha S(t) = 0$, $D^\alpha I(t) = 0$, $D^\alpha Q(t) = 0$ and $D^\alpha R(t) = 0$. It is apparent that system (1.1) always possesses a disease-free equilibrium $E_1(\frac{A}{d}, 0, 0, 0)$. In order to derive the basic reproduction number $\mathcal{R}_0$ of system (1.1), we employ the next generation matrix method as presented in [30].

If $x = (I, Q, R)^\top$ then when τ equals zero, the original system can be expressed as

$$\frac{dx}{dt} = \mathcal{F}(x) - \mathcal{V}(x), \tag{4.1}$$

where

$$\mathcal{F}(x) = \begin{pmatrix} \beta SI \\ 0 \\ 0 \end{pmatrix},$$

$$\mathcal{V}(x) = \begin{pmatrix} (d+a+\gamma+\sigma)I \\ -\sigma I + (d+b+p)Q \\ -\sigma I - pQ + dR \end{pmatrix}.$$

We can get

$$F = \begin{pmatrix} \frac{\beta A}{d} & 0 & 0 \\ 0 & 0 & 0 \\ 0 & 0 & 0 \end{pmatrix},$$

$$V = \begin{pmatrix} \mu+\delta+\sigma & 0 & 0 \\ -\sigma & d+b+p & 0 \\ -\gamma & -p & d \end{pmatrix}.$$

The next generation matrix for model (1.1) is

$$FV^{-1} = \begin{pmatrix} \frac{A\beta}{d(\gamma+d+a+\sigma)} & 0 & 0 \\ 0 & 0 & 0 \\ 0 & 0 & 0 \end{pmatrix}.$$

The spectral radius $\rho(FV^{-1}) = \dfrac{A\beta}{d(\gamma+d+a+\sigma)}$. According to Theorem 2 in [30], the basic reproduction number of system (1.1) is

$$\mathcal{R}_0 = \frac{A\beta}{d(\gamma+d+a+\sigma)}.$$

Theorem 4.1 If $\mathcal{R}_0 > 1$, system (1.1) has a unique endemic equilibrium E^*. If $\mathcal{R}_0 < 1$, there is no endemic equilibrium of system (1.1).

Proof. To obtain the endemic equilibrium E^* of system (1.1), we need to impose the right side of system (1.1) to be equal to 0. In other words, the equilibrium $E^*(S^*, I^*, Q^*, R^*)$ should be satisfied the following equations

$$\begin{cases} A - \beta S^* I^* - dS^* = 0, \\ \beta S^* I^* - (d+a+\gamma+\sigma)I^* = 0, \\ \sigma I^* - (d+b+p)Q^* = 0, \\ \gamma I^* + pQ^* - dR^* = 0. \end{cases} \tag{4.2}$$

From above, we can obtain

$$S^* = \frac{\gamma+d+a+\sigma}{\beta}, Q^* = \frac{\sigma}{d+b+p}I^*, R^* = \frac{\gamma I^* + pQ^*}{d} \tag{4.3}$$

and

$$I^* = \frac{d}{\beta}(1 - \frac{1}{\mathcal{R}_0}).$$

It is obvious that $S^* > 0$. When $\mathcal{R}_0 > 1$, $I^* > 0$. Hence, $Q^* > 0$, $R^* > 0$. Then, system (1.1) has a unique endemic equilibrium. And when $\mathcal{R}_0 < 1$, $I^* < 0$, there is no endemic equilibrium of system (1.1).

In the following, we will discuss the local asymptotical stability of the disease-free equilibrium E_0, the endemic equilibrium E^* for system (1.1) and the existence of Hopf bifurcation around the endemic equilibrium E^*.

To discuss the local asymptotical stability of system (1.1), we have to linearize it. Let us consider the following coordinate transformation

$$x(t) = S(t) - \bar{S},\ y(t) = I(t) - \bar{I},\ z(t) = Q(t) - \bar{Q},\ w(t) = R(t) - \bar{R},$$

where $(\bar{S}, \bar{I}, \bar{Q}, \bar{R})$ denotes any equilibrium of system (1.1). So we can obtain the corresponding linearized system is of the form

$$\begin{cases} D^\alpha x(t) = -dx(t) - \beta\bar{I}x(t-\tau) - \beta\bar{S}y(t-\tau), \\ D^\alpha y(t) = \beta\bar{I}x(t-\tau) + \beta\bar{S}y(t-\tau) - (d+a+\sigma+\gamma)y(t), \\ D^\alpha z(t) = \sigma y(t) - (d+b+p)z(t), \\ D^\alpha w(t) = \gamma y(t) + pz(t) - dw(t). \end{cases} \tag{4.4}$$

Taking Laplace transform on both sides of (4.4), yields

$$\begin{aligned} & s^\alpha S(s) - s^{\alpha-1}x(0) = -dS(s) - \beta\bar{I}e^{-s\tau}[S(s) + \int_{-\tau}^0 e^{-st}\varphi_1(t)dt] \\ & \quad -\beta\bar{S}e^{-s\tau}[I(s) + \int_{-\tau}^0 e^{-st}\varphi_2(t)dt], \\ & s^\alpha I(s) - s^{\alpha-1}y(0) = \beta\bar{S}e^{-s\tau}[I(s) + \int_{-\tau}^0 e^{-st}\varphi_2(t)dt] \\ & \quad +\beta\bar{I}e^{-s\tau}[S(s) + \int_{-\tau}^0 e^{-st}\varphi_1(t)dt] - (d+a+\sigma+\gamma)I(s), \\ & s^\alpha Q(s) - s^{\alpha-1}z(0) = \sigma I(s) - (d+b+p)Q(s), \\ & s^\alpha R(s) - s^{\alpha-1}w(0) = \gamma I(s) + pQ(s) - dR(s). \end{aligned} \tag{4.5}$$

Here, $S(s), I(s), Q(s), R(s)$ are the Laplace transform of $x(t), y(t), z(t), w(t)$, respectively. The above system (4.5) can be written as follows

$$\Delta(s) \cdot \begin{pmatrix} S(s) \\ I(s) \\ Q(s) \\ R(s) \end{pmatrix} = \begin{pmatrix} b_1(s) \\ b_2(s) \\ b_3(s) \\ b_4(s) \end{pmatrix},$$

where

$$\Delta(s) = \begin{pmatrix} s^\alpha + \beta\bar{I}e^{-\lambda\tau} + d & \beta\bar{S}e^{-\lambda\tau} & 0 & 0 \\ \beta\bar{I}e^{-\lambda\tau} & s^\alpha - \beta\bar{S}e^{-\lambda\tau} + (d+s+\sigma+\gamma) & 0 & 0 \\ 0 & -\sigma & s^\alpha + d + b + p & 0 \\ 0 & -\gamma & -p & s^\alpha + d \end{pmatrix}$$

and

$$\begin{aligned} b_1(s) &= s^{\alpha-1}x(0) - \beta\bar{I}e^{-s\tau}\int_{-\tau}^{0} e^{-st}\varphi_1(t)dt - \beta\bar{S}e^{-s\tau}\int_{-\tau}^{0} e^{-st}\varphi_2(t)dt,\\ b_2(s) &= s^{\alpha-1}y(0) + \beta\bar{I}e^{-s\tau}\int_{-\tau}^{0} e^{-st}\varphi_1(t)dt + \beta\bar{S}e^{-s\tau}\int_{-\tau}^{0} e^{-st}\varphi_2(t)dt,\\ b_3(s) &= s^{\alpha-1}z(0),\\ b_4(s) &= s^{\alpha-1}w(0). \end{aligned}$$

Theorem 4.2 If $\mathcal{R}_0 < 1$, then the disease-free equilibrium E_1 of system (1.1) is locally asymptotically stable for all $\tau \geq 0$.

Proof. The characteristic matrix at $E_1(\frac{A}{d}, 0, 0, 0)$ is

$$\Delta_1(s) = \begin{pmatrix} s^\alpha + d & \frac{\beta A}{d}e^{-s\tau} & 0 & 0\\ 0 & s^\alpha - \frac{\beta A}{d}e^{-s\tau} + (d+a+\sigma+\gamma) & 0 & 0\\ 0 & -\sigma & s^\alpha + d + b + p & 0\\ 0 & -\gamma & -p & s^\alpha + d \end{pmatrix}.$$

Then the characteristic equation at the disease-free equilibrium $E_1(\frac{A}{d}, 0, 0, 0)$ is

$$(s^\alpha + d)^2(s^\alpha + d + b + p)\left[s^\alpha + (d+a+\sigma+\gamma) - \frac{\beta A}{d}e^{-s\tau}\right] = 0. \tag{4.6}$$

When $\tau = 0$, the characteristic equation can be translated into

$$(s^\alpha + d)^2(s^\alpha + d + b + p)\left[s^\alpha + (d+a+\sigma+\gamma) - \frac{\beta A}{d}\right] = 0. \tag{4.7}$$

Let $s^\alpha = \lambda$, Eq. (4.7) can be rewritten as $(\lambda+d)^2(\lambda+d+b+p)[\lambda+(d+a+\sigma+\gamma)-\frac{\beta A}{d}] = 0$. Its characteristic root is $\lambda_{1,2} = -d$, $\lambda_3 = -(d+b+p)$, $\lambda_4 = \frac{\beta A}{d} - (d+a+\sigma+\gamma) = (\mathcal{R}_0-1)(d+a+\sigma+\gamma)$. Obviously, $|\arg(\lambda_1)| = |\arg(\lambda_2)| = |\arg(\lambda_3)| = \pi > \frac{\alpha\pi}{2}$. $|\arg(\lambda_4)| = \pi > \frac{\alpha\pi}{2}$ when the basic reproduction number $\mathcal{R}_0 < 1$. Hence, all the eigenvalues λ_i of $\Delta_1(s)$ satisfy $|\arg(\lambda_i)| = \pi > \frac{\alpha\pi}{2}$, $i = 1, 2, 3, 4$. According to the Lemma 2.2, the disease-free equilibrium E_1 is locally asymptotically stable when $\mathcal{R}_0 < 1$.

When $\tau \neq 0$, since the first two factors of the left side of Eq. (4.7) do not contain time delay τ, we only need to consider the third factor

$$s^\alpha - \frac{\beta A}{d}e^{-s\tau} + (d+a+\sigma+\gamma) = 0. \tag{4.8}$$

Assume $s = i\omega = \omega(\cos\frac{\pi}{2} + i\sin\frac{\pi}{2})$ $(\omega > 0)$, then s is substituted, in (4.8), we get

$$(i\omega)^\alpha - \frac{\beta A}{d}e^{-i\omega\tau} + (d+a+\sigma+\gamma) = 0. \tag{4.9}$$

Separating the imaginary parts and real parts, it leads to

$$\begin{cases} \omega^\alpha \cos\dfrac{\alpha\pi}{2} + (d+a+\sigma+\gamma) = \dfrac{\beta A}{d}\cos\omega\tau, \\ \omega^\alpha \sin\dfrac{\alpha\pi}{2} = -\dfrac{\beta A}{d}\sin\omega\tau. \end{cases} \tag{4.10}$$

Squaring and adding both sides of this equation, we can obtain

$$\omega^{2\alpha} + 2(d+a+\sigma+\gamma)\cos\frac{\alpha\pi}{2}\omega^\alpha + \left(d+a+\sigma+\gamma+\frac{\beta A}{d}\right)(d+a+\sigma+\gamma)(1-\mathcal{R}_0) = 0. \tag{4.11}$$

Obviously, $2(d+a+\sigma+\gamma)\cos\frac{\alpha\pi}{2} \geq 0$ and our assumption that $\mathcal{R}_0 < 1$, then the Eq. (4.11) has no positive roots. Which ensures that Eq. (4.7) has no purely imaginary roots if $\mathcal{R}_0 < 1$. According to Lemma 2.2, the equilibrium E_1 is locally asymptotically stable for any delay $\tau \geq 0$ if $\mathcal{R}_0 < 1$. The proof is completed.

Next, we discuss the local stability and bifurcation results at the endemic equilibrium point E^*. When $\mathcal{R}_0 > 1$, the endemic equilibrium point E^* exists. The characteristic matrix at E^* is

$$\Delta_2(s) = \begin{pmatrix} s^\alpha + \beta I^* e^{-\lambda\tau} + d & \beta S^* e^{-\lambda\tau} & 0 & 0 \\ \beta I^* e^{-\lambda\tau} & s^\alpha - \beta S^* e^{-\lambda\tau} + (d+s+\sigma+\gamma) & 0 & 0 \\ 0 & -\sigma & s^\alpha + d + b + p & 0 \\ 0 & -\gamma & -p & s^\alpha + d \end{pmatrix}.$$

The associated characteristic equation of system (1.1) at E^* can be described as

$$s^{4\alpha} + \kappa_1 s^{3\alpha} + \kappa_2 s^{2\alpha} + \kappa_3 s^\alpha + \kappa_4 + (\kappa_5 s^{3\alpha} + \kappa_6 s^{2\alpha} + \kappa_7 s^\alpha + \kappa_8)e^{-s\tau} = 0, \tag{4.12}$$

where

$$\begin{aligned}
\kappa_1 &= 4d + b + p + \gamma + a + \sigma, \\
\kappa_2 &= 3da + ap + 3bd + ab + 6d^2 + 3d\sigma + 3d\gamma + p\gamma + b\gamma + \sigma p + 3pd + \sigma b, \\
\kappa_3 &= 2d\sigma b + 3d^2\gamma + 2d\sigma p + 4d^3 + 2dap + 3d^2 a \\
&\qquad + 3d^2\sigma + 2d\gamma b + 3d^2 b + 3d^2 p + 2dab + 2d\gamma p, \\
\kappa_4 &= d^3 p + d^3\gamma + d^2 ab + d^2\sigma p + d^3\sigma + d^4 + d^2\sigma b \\
&\qquad + d^2\gamma b + d^2\gamma p + d^2 ap + d^3 b + d^3 a, \\
\kappa_5 &= \beta I^* - \beta S^*, \\
\kappa_6 &= i\beta\gamma + I^*\beta\sigma + i\beta p - \beta S^* p - \beta S b + I^*\beta b - 3\beta S^* d + 3I^*\beta d + i\beta a, \\
\kappa_7 &= I^*\beta\sigma b + 2I^*\beta ad + 2I^*\beta\gamma d + I^*\beta\sigma pd^2 + 2I^*\beta\sigma d - 3d^2\beta S^* - 2\beta S^* pd \\
&\qquad + 3I^*\beta + 2I^*\beta pd + I^*\beta ab + 2I^*\beta bd + I^*\beta\gamma p - 2d\beta S^* b + I^*\beta ap + I^*\beta\gamma b, \\
\kappa_8 &= -d^3\beta S^* + I^*\beta\gamma d^2 + I^*\beta abd - d^2\beta S^* p + I^*\beta\sigma bd + I^*\beta\gamma pd + I^*\beta d^2 p - d^2\beta S^* b \\
&\qquad + I^*\beta d^2 b + I^*\beta\sigma d^2 + I^*\beta\gamma bd + I^*\beta ad^2 + I^*\beta apd + I^*\beta d^3 + I^*\beta\sigma pd.
\end{aligned}$$

Case 1. When $\tau = 0$, Eq. (4.12) becomes

$$(s^\alpha)^4 + (\kappa_1 + \kappa_5)(s^\alpha)^3 + (\kappa_2 + \kappa_6)(s^\alpha)^2 + (\kappa_3 + \kappa_7)s^\alpha + \kappa_4 + \kappa_8 = 0.$$

On the basis of Routh-Hurwitz theorem, the endemic equilibrium point E^* is locally asymptotically stable if

$$\begin{array}{l} \kappa_1 + \kappa_5 > 0,\ \kappa_2 + \kappa_6 > 0,\ \kappa_3 + \kappa_7 > 0,\ \kappa_4 + \kappa_8 > 0, \\ (\kappa_1 + \kappa_5)(\kappa_2 + \kappa_6)(\kappa_3 + \kappa_7) > (\kappa_3 + \kappa_7)^2 + (\kappa_1 + \kappa_5)^2(\kappa_4 + \kappa_8). \end{array} \tag{4.13}$$

Case 2. When $\tau > 0$, let $s = i\omega = \omega(\cos\frac{\pi}{2} + i\sin\frac{\pi}{2})$ $(\omega > 0)$ be a root of Eq. (4.12). Substitute s in (4.12), we obtain

$$\begin{array}{l} \omega^{4\alpha}(\cos 2\alpha\pi + i\sin 2\alpha\pi) + \kappa_1\omega^{3\alpha}(\cos\frac{3\alpha\pi}{2} + i\sin\frac{3\alpha\pi}{2}) \\ \quad +\kappa_2\omega^{2\alpha}(\cos\alpha\pi + i\sin\alpha\pi) + \kappa_3\omega^{\alpha}(\cos\frac{\alpha\pi}{2} + i\sin\frac{\alpha\pi}{2}) + \kappa_4 \\ \quad +[\kappa_5\omega^{3\alpha}(\cos\frac{3\alpha\pi}{2} + i\sin\frac{3\alpha\pi}{2}) + \kappa_6\omega^{2\alpha}(\cos\alpha\pi + i\sin\alpha\pi) \\ \quad +\kappa_7\omega^{\alpha}(\cos\frac{\alpha\pi}{2} + i\sin\frac{\alpha\pi}{2}) + \kappa_8](\cos\omega\tau - i\sin\omega\tau) = 0. \end{array}$$

Separating the real and imaginary parts of (4), yields

$$\begin{cases} R_2\cos(\omega\tau) + I_2\sin(\omega\tau) = -R_1, \\ I_2\cos(\omega\tau) - R_2\sin(\omega\tau) = -I_1, \end{cases} \tag{4.14}$$

where

$$\begin{aligned} R_1 &= \omega^{4\alpha}\cos(2\alpha\pi) + \kappa_1\omega^{3\alpha}\cos\left(\frac{3\alpha\pi}{2}\right) + \kappa_2\omega^{2\alpha}\cos(\alpha\pi) + \kappa_3\omega^{\alpha}\cos\left(\frac{\alpha\pi}{2}\right) + \kappa_4, \\ R_2 &= \kappa_5\omega^{3\alpha}\cos\left(\frac{3\alpha\pi}{2}\right) + \kappa_6\omega^{2\alpha}\cos(\alpha\pi) + \kappa_7\omega^{\alpha}\cos\left(\frac{\alpha\pi}{2}\right) + \kappa_8, \\ I_1 &= \omega^{4\alpha}\sin(2\alpha\pi) + \kappa_1\omega^{3\alpha}\sin\left(\frac{3\alpha\pi}{2}\right) + \kappa_2\omega^{2\alpha}\sin(\alpha\pi) + \kappa_3\omega^{\alpha}\sin\left(\frac{\alpha\pi}{2}\right), \\ I_2 &= \kappa_5\omega^{3\alpha}\sin\left(\frac{3\alpha\pi}{2}\right) + \kappa_6\omega^{2\alpha}\sin(\alpha\pi) + \kappa_7\omega^{\alpha}\sin\left(\frac{\alpha\pi}{2}\right). \end{aligned} \tag{4.15}$$

From Eq. (4.14), we have

$$\begin{aligned} \cos(\omega\tau) &= -\frac{R_1R_1 + I_1I_2}{R_2^2 + I_2^2} \triangleq F(\omega), \\ \sin(\omega\tau) &= \frac{R_2I_1 - R_1I_2}{R_2^2 + I_2^2} \triangleq G(\omega). \end{aligned} \tag{4.16}$$

It is obvious that $\cos^2(\omega\tau) + \sin^2(\omega\tau) = 1$, and

$$\omega^{8\alpha} + \mathcal{M} + \mathcal{N} = 0, \tag{4.17}$$

where $\mathcal{M}$ is a polynomial containing $\omega^{7\alpha}$, $\omega^{6\alpha}$, $\omega^{5\alpha}$, $\omega^{4\alpha}$, $\omega^{3\alpha}$, $\omega^{2\alpha}$, ω^{α}, and $\mathcal{N}$ is a constant.

Let

$$h(\omega) = \omega^{8\alpha} + \mathcal{M} + \mathcal{N}.$$

Suppose that $\mathcal{N} < 0$. Thus, $h(\omega)$ has at least one positive root. The delay τ is regarded as a bifurcation parameter. Let $s(\omega) = \xi(\tau) + i\omega(\tau)$ be the eigenvalue of () such that for some initial value of the bifurcation parameter τ_0 we have $\xi(\tau_0) = 0$, $\omega(\tau_0) = \omega_0$. Without loss of generality, we assume $\omega(0) > 0$. From (4.16), we can conclude

$$\tau_j = \frac{1}{\omega_0}[\arccos F(\omega) + 2j\pi], \quad j = 0, 1, 2, \cdots,$$

where

$$\tau_0 = \min \tau_j, \quad j = 0, 1, 2, \cdots.$$

It is imperative that the following lemma is useful and needed.

Lemma 4.1 If $\mathcal{N} < 0$, then Hopf bifurcation occurs provided $h'(\omega_0) \neq 0$.

Proof. Differentiating both sides of Eq. (4.12) with respected to τ, it can be obtained that

$$\begin{aligned}&(4\alpha s^{4\alpha-1} + 3\alpha\kappa_1 s^{3\alpha-1} + 2\alpha\kappa_2 s^{2\alpha-1} + \alpha\kappa_3 s^{\alpha-1})\frac{ds}{s\tau}\\ &+(3\kappa_5\alpha s^{3\alpha-1} + 2\alpha\kappa_6 s^{2\alpha-1} + \alpha\kappa_7 s^{\alpha-1})e^{-s\tau}\tfrac{ds}{s\tau}\\ &+(\kappa_5\alpha s^{3\alpha} + \kappa_6 s^{2\alpha} + \kappa_7 s^{\alpha} + \kappa_8)e^{-s\tau}(-\tau\tfrac{ds}{d\tau} - s) = 0.\end{aligned} \tag{4.18}$$

Hence, we can get

$$\begin{aligned}\left(\frac{ds}{d\tau}\right)^{-1} &= \frac{4\alpha s^{4\alpha-1} + 3\alpha\kappa_1 s^{3\alpha-1} + 2\alpha\kappa_2 s^{2\alpha-1} + \alpha\kappa_3 s^{\alpha-1}}{s(\kappa_5\alpha s^{3\alpha} + \kappa_6 s^{2\alpha} + \kappa_7 s^{\alpha} + \kappa_8)e^{-s\tau}}\\ &\quad + \frac{(3\kappa_5\alpha s^{3\alpha-1} + 2\alpha\kappa_6 s^{2\alpha-1} + \alpha\kappa_7 s^{\alpha-1})e^{-s\tau}}{s(\kappa_5\alpha s^{3\alpha} + \kappa_6 s^{2\alpha} + \kappa_7 s^{\alpha} + \kappa_8)e^{-s\tau}} - \frac{\tau}{s}\\ &= \frac{4\alpha s^{4\alpha-1} + 3\alpha\kappa_1 s^{3\alpha-1} + 2\alpha\kappa_2 s^{2\alpha-1} + \alpha\kappa_3 s^{\alpha-1}}{s(\kappa_5\alpha s^{3\alpha} + \kappa_6 s^{2\alpha} + \kappa_7 s^{\alpha} + \kappa_8)e^{-s\tau}}\\ &\quad + \frac{3\kappa_5\alpha s^{3\alpha-1} + 2\alpha\kappa_6 s^{2\alpha-1} + \alpha\kappa_7 s^{\alpha-1}}{s(\kappa_5\alpha s^{3\alpha} + \kappa_6 s^{2\alpha} + \kappa_7 s^{\alpha} + \kappa_8)} - \frac{\tau}{s}.\end{aligned} \tag{4.19}$$

Substituting $s = i\omega_0$ into Eq. (4.19), we obtain

$$\begin{aligned} Re\left[\left(\frac{ds}{d\tau}\right)^{-1}\Big|_{\tau=\tau_0}\right] &= \frac{4\alpha(i\omega_0)^{4\alpha-1} + 3\alpha\kappa_1(i\omega_0)^{3\alpha-1} + 2\alpha\kappa_2(i\omega_0)^{2\alpha-1} + \alpha\kappa_3(i\omega_0)^{\alpha-1}}{(i\omega_0)(\kappa_5\alpha(i\omega_0)^{3\alpha} + \kappa_6(i\omega_0)^{2\alpha} + \kappa_7(i\omega_0)^{\alpha} + \kappa_8)e^{-s\tau}} \\ &\quad + \frac{3\kappa_5\alpha s^{3\alpha-1} + 2\alpha\kappa_6 s^{2\alpha-1} + \alpha\kappa_7 s^{\alpha-1}}{s(\kappa_5\alpha s^{3\alpha} + \kappa_6 s^{2\alpha} + \kappa_7 s^{\alpha} + \kappa_8)} - \frac{\tau}{s} \\ &= \frac{h'(\omega_0)}{2\omega_0 G}, \end{aligned}$$

where

$$\begin{aligned} G = &\left(\kappa_1\omega_0^{3\alpha}\cos\frac{(3\alpha+1)\pi}{2} + \kappa_2\omega_0^{2\alpha}\cos\frac{(2\alpha+1)\pi}{2} + \kappa_3\omega_0^{\alpha}\cos\frac{(\alpha+1)\pi}{2}\right)^2 \\ &+\left(\kappa_1\omega_0^{3\alpha}\sin\frac{(3\alpha+1)\pi}{2} + \kappa_2\omega_0^{2\alpha}\sin\frac{(2\alpha+1)\pi}{2} + \kappa_3\omega_0^{\alpha}\sin\frac{(\alpha+1)\pi}{2} + \kappa_4\right)^2. \end{aligned}$$

Then,

$$\operatorname{sign}\left\{\frac{\mathrm{d}Re(\lambda)}{d\tau}\Big|_{\tau=\tau_0}\right\} = \operatorname{sign}\left\{Re\left[\left(\frac{ds}{d\tau}\right)^{-1}\Big|_{\tau=\tau_0}\right]\right\} = \operatorname{sign}\{h'(\omega_0)\}.$$

Obviously, if $h'(\omega_0) \neq 0$ the transversality condition holds, and Hopf bifurcation occurs at $\tau = \tau_0$.

Theorem 4.3 When $\mathcal{R}_0 > 1$ and $h'(\omega_0) \neq 0$, the endemic equilibrium point E^* of system (1.1) is locally asymptotically stable if $\tau < \tau_0$ and unstable if $\tau > \tau_0$, where $\tau_0 = \min\{\tau_j, j = 0, 1, 2, 3, \cdots\}$.

5. Numerical simulations

In this section, several illustrative numerical examples are presented to confirm the theoretical results and to examine the dynamical behavior of system (1.1). From Section 4, we can find that delay τ and fractional-order α are the important factors which affect the convergence speed of solutions. We select parameters as follows

$$A = 10,\ \beta = 0.002,\ d = 0.01,\ \gamma = 0.2,\ p = 0.6,\ a = 0.01,\ b = 0.2,\ \sigma = 0.1$$

with initial conditions $S(0) = 160$, $I(0) = 25$, $Q(0) = 3$, $R(0) = 720$. We can calculate $\mathcal{R}_0 = 6.25 > 1$. System (1.1) have three equilibria $E_1(1000, 0, 0, 0)$ and $E^*(160.00,\ 26.25,\ 3.24,\ 719.44)$. We only discuss the stability of E^*.

(1) $\alpha = 0.98$ **and** $\tau = 3$**.**

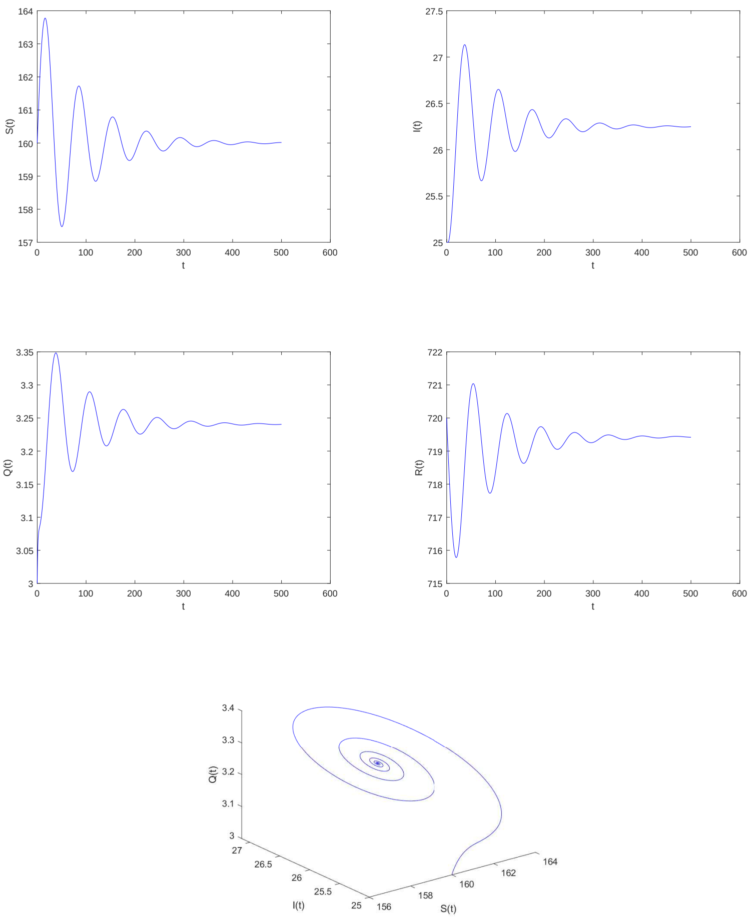

Figure 1: Time evolution of all the population for the model (1.1) with $\alpha = 0.98$ and $\tau = 3.0$.

We can calculate $\tau^* = 9.68$ from (4.14). Obviously, $\tau < \tau^* = 8.23$. From Theorem 4.4, we can obtain that E^* is locally asymptotically stable (See Fig. 1).

(2) $\alpha = 0.98$ **and** $\tau = 10.1$**.**

It is to see that $\tau > \tau^* = 9.68$. From Theorem 4.4, we can find that E^* is unstable and Hopf bifurcation occurs (See Fig. 2).

(3) $\alpha = 0.90$ **and** $\tau = 10.1$**.**

We can calculate $\tau^* = 12.32$ and $\tau < \tau^*$. Then E^* is locally asymptotically stable (See Fig. 3).

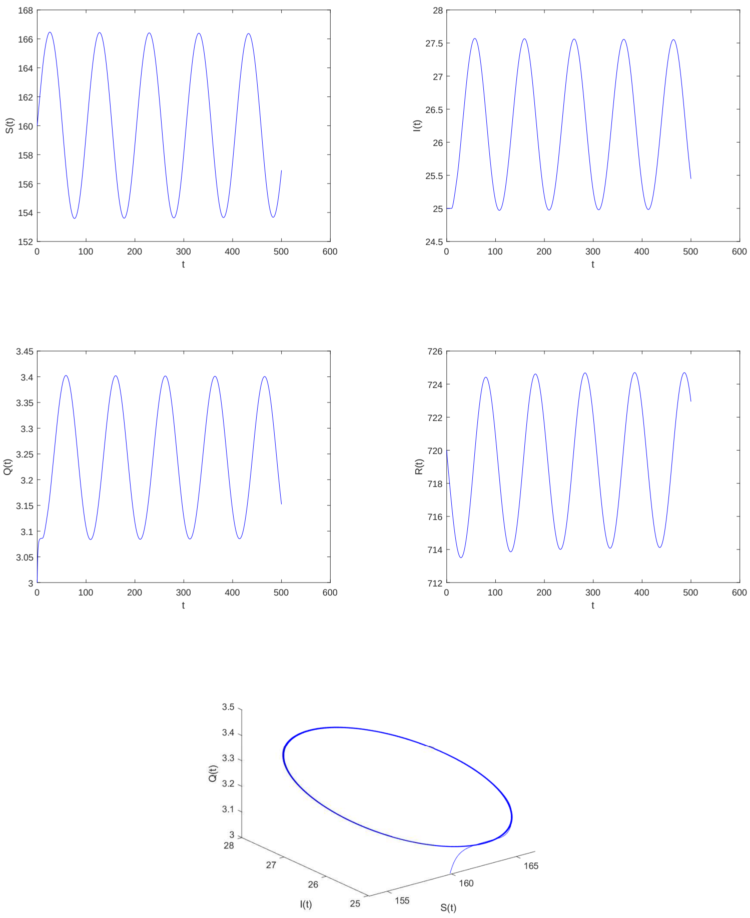

Figure 2: Time evolution of all the population for the model (1.1) with $\alpha = 0.98$ and $\tau = 10.1$.

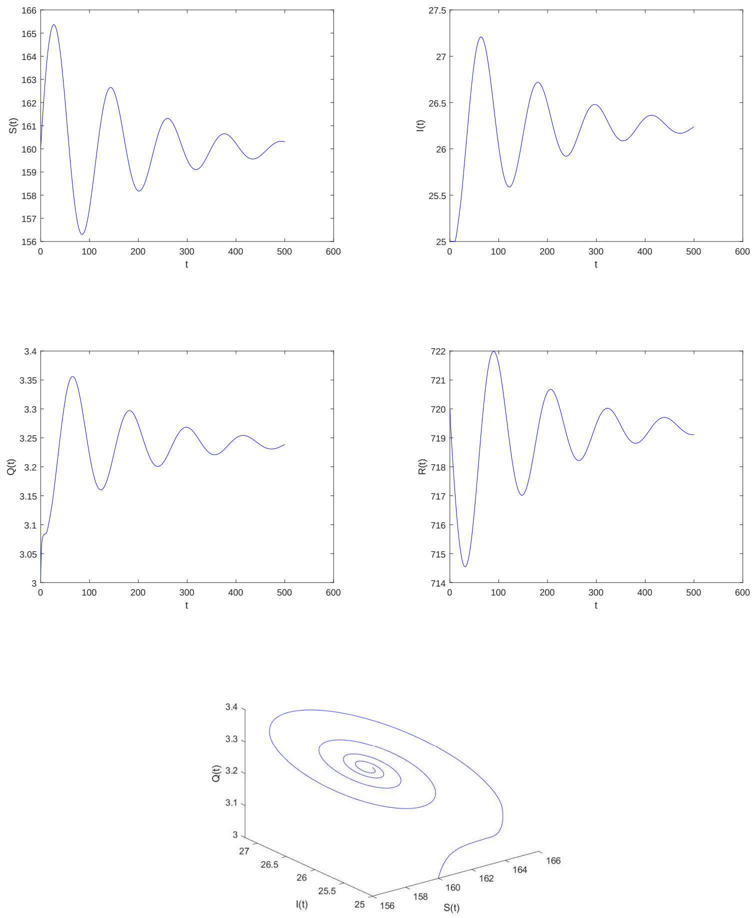

Figure 3: Time evolution of all the population for the model (1.1) with $\alpha = 0.90$ and $\tau = 10.1$.

6. Conclusion

In this work, we studied a fractional-order SIQR epidemic model with delay for COVID-19 pandemic. The dynamical behavior of system (1.1) is studied. Local stability of the equilibria for system (1.1) and Hopf bifurcation are analyzed. The disease-free equilibrium E_1 of system (1.1) is locally asymptotically stable for all $\tau \geq 0$ when $\mathcal{R}_0 < 1$. When $\mathcal{R}_0 > 1$ and $\tau = 0$, the endemic equilibrium is locally asymptotically stable. According to Theorem 4.3, when $\mathcal{R}_0 > 1$ and the conditions of Theorem 4.3 satisfied, the stability of the endemic equilibrium changes at Hopf bifurcation point τ^*. To validate the accuracy of the theoretical analysis, suitable parameters were chosen for numerical simulations. The results demonstrated that the threshold of time delay was indeed a pivotal point in the Hopf bifurcation of the fractional order COVID-19 epidemic model. The size of the time lag, given the parameter values, is a crucial factor influencing the stability of the system and directly affects the effectiveness of the regulation and control system in transitioning from a infected state to a healthy state. Moreover, the numerical simulation revealed that variations in the fractional order led to changes in the critical value of the Hopf bifurcation, further substantiating the efficacy of fractional order in controlling the stability domain of the model.

References

[1] Luo X.F., Feng S., Yang J., et al. Nonpharmaceutical interventions contribute to the control of COVID-19 in China based on a pairwise model. Infectious Disease Modelling, 2021, 6: 643-663.

[2] Tang X., Wu C., Li X., et al. On the origin and continuing evolution of SARS-CoV-2. National Science Review, 2020, 7(6): 1012-1023.

[3] Chinazzi M., Davis J.T., Ajelli M., et al. The effect of travel restrictions on the spread of the 2019 novel coronavirus (COVID-19) outbreak. Science. 2020, 368(6489): 395-400.

[4] Peeri N.C., Shrestha N., Rahman M.S., et al. The SARS, MERS and novel coronavirus (COVID-19) epidemics, the newest and biggest global health threats: what lessons have we learned? International Journal of Epidemiology. 2020, 49(3): 717-726.

[5] Hiroshi N.,Tetsuro K., Takeshi M., et al. Estimation of the asymptomatic ratio of novel coronavirus infections (COVID-19). International Journal of Infenctious Diseases. 2020, 94(2): 154-155.

[6] Li Q., Xiao Y.N., Wu J.H., Tang S.Y., Modelling COVID-19 epidemic with time delay and analyzing the strategy of confirmed cases-driven contact tract-

ing following by quarantine (in Chinese), Acta Mathematicae Applicatae Sinica, 2020, 43(2):238-250.

[7] Peter O.J., Panigoro H.S., Abidemi A., et al. Mathematical model of COVID-19 pandemic with double dose vaccination. Acta Biotheoretica, 2023, 71(2): 9.

[8] Gao S, Binod P, Chukwu C W, et al. A mathematical model to assess the impact of testing and isolation compliance on the transmission of COVID-19. Infectious Disease Modelling, 2023, 8(2): 427-444.

[9] Danane J., Hammouch Z., Allali K., et al. A fractional-order model of coronavirus disease 2019 (COVID-19) with governmental action and individual reaction. Mathematical Methods in the Applied Sciences, 2023, 46(7): 8275-8288.

[10] Butt A.I.K., Imran M., Chamaleen D.B.D., et al. Optimal control strategies for the reliable and competitive mathematical analysis of Covid-19 pandemic model. Mathematical Methods in the Applied Sciences, 2023, 46(2): 1528-1555.

[11] Sokolov A.V., Sokolova L.A. COVID-19 dynamic model: balanced identification of general biological and country specific features. Procedia Computer Science, 2020, 178: 301-310.

[12] Lazzizzera, I. An analytic approximate solution of the SIR model. Applied Mathematics, 2021, 12: 58-73.

[13] Podlubny I., Fractional Differential Equations, Academic Press, New York, 1999.

[14] Dai Y., Wei Y., Hu Y., et al. Modulating function-based identification for fractional order systems. Neurocomputing, 2016, 173: 1959-1966.

[15] Wei Y., Tse P.W., Yao Z., et al. Adaptive backstepping output feedback control for a class of nonlinear fractional order systems. Nonlinear Dynamics, 2016, 86: 1047-1056.

[16] Zarin R., Khan A., Yusuf A., et al. Analysis of fractional COVID-19 epidemic model under Caputo operator. Mathematical Methods in the Applied Sciences, 2023, 46(7): 7944-7964.

[17] Arshad S., Siddique I., Nawaz F., et al. Dynamics of a fractional order mathematical model for COVID-19 epidemic transmission. Physica A: Statistical Mechanics and its Applications, 2023, 609: 128383.

[18] Ruan S., Wang W.. Dynamical behavior of an epidemic model with a nonlinear incidence rate. Journal of Differential Equations, 2003, 188(1): 135-163.

[19] Xiao D., Ruan S.. Global analysis of an epidemic model with nonmonotone incidence rate. Mathematical Biosciences, 2007, 208(2): 419-429.

[20] Tchuenche J.M., Nwagwo A., Levins R., Global behaviour of an SIR epidemic model with time delay. Mathematical Methods in the Applied Sciences, 2007, 30(6): 733-749.

[21] Wang W., Global behavior of an SEIRS epidemic model with time delays. Applied Mathematics Letters, 2002, 15(4): 423-428.

[22] Liu L., A delayed SIR model with general nonlinear incidence rate. Advances in Difference Equations, 2015, 2015(1): 1-11.

[23] Vinitsky S.I., Gusev A.A., Derbov V.L., et al. Reduced SIR model of COVID-19 pandemic. Computational Mathematics and Mathematical Physics, 2021, 61(3): 376-387.

[24] Pen'kov F.M., Derbov V.L., Chuluunbaatar G., et al. Approximate Solutions of the RSIR Model of COVID-19 Pandemic. A. Byrski et al. (Eds.): ANTICOVID 2021, IFIP AICT 2021; 616: 53-64.

[25] Li C.P., Zhao Z.G., Asymptotical stability analysis of linear fractional diferential systems, Journal of Shanghai University (English Edition), 2009, 13(3): 197-206.

[26] Deng W.H., Li C.P., L*ü* J.H., Stability analysis of linear fractional diferential system with multiple time delays, Nonlinear Dynamics, 2007, 48(4): 409-416.

[27] Li H.L., Zhang L., Hu C., Jiang Y.L., Teng Z.D., Dynamical analysis of a fractional-order predator-prey model incorporating a prey refuge, Journal of Applied Mathematics and Computing, 2017, 54(1-2): 435-449.

[28] Odibat Z.M., Shawagfeh N.T., Generalized Taylors formula, Applied Mathematics and Computation, 2007, 186: 286-293.

[29] Boukhouima A., Hattaf K., Yousfi N., Dynamics of a fractional order HIV infection model with specific functional response and cure rate, International Journal of Differential Equations, 2017, 2017: 8372140.

[30] van den Driessche P., Watmough J., Reproduction numbers and sub-threshold endemic equilibria for compartmental models of disease transmission, Mathematical Biosciences, 2007, 180: 29-48.

Competing interests

The authors declare that they have no competing interests.

Author's contributions

Xueyong Zhou conceived the model and made the numerical simulations. Yaozong Deng wrote the paper. All authors read and approved the manuscript.

Acknowledgements

This work is sponsored by the Natural Science Foundation of Henan (222300420521) and Nanhu Scholars Program for Young Scholars of XYNU.